Abnormal magnetoresistance effect in the Nb/Si superconductor–semiconductor heterojunction

Zhi-Wei Hu(胡志伟)[1,2,†] and Xiang-Gang Qiu(邱祥冈)[1,2,3]

[1] *Beijing National Laboratory for Condensed Matter Physics, Institute of Physics, Chinese Academy of Sciences, Beijing* 100190, *China*
[2] *School of Physical Sciences, University of Chinese Academy of Sciences, Beijing* 100049, *China*
[3] *Collaborative Innovation Center of Quantum Matter, Beijing* 100084, *China*

(Received 4 July 2022; revised manuscript received 17 August 2022; accepted manuscript online 19 August 2022)

Ultrathin superconducting Nb films of about 8 nm thick have been deposited on heavily doped Si substrates through DC magnetron sputtering and then the high-quality Nb/Si superconductor–semiconductor heterojunctions have been fabricated by electron beam lithography and reactive ion etching. An abnormal magnetoresistance effect, which manifests itself as a zero field resistance peak under a magnetic field applied perpendicular to the interface, has been distinctly observed when the Nb film is in the superconductiing state. By considering the heterojunction interface being equivalent to the structure of superconductor–barrier layer–superconductor configuration, we could generally understand this unusual effect based on the Andreev reflection mechanism. Our results can be of help for the future development on compatibility and scalability of the silicon-based nanoscale superconducting devices for integrated circuits and superconducting quantum electronics.

Keywords: superconductor, magnetoresistance, heterojunction

PACS: 74.81.Bd, 75.47.–m, 73.40.Lq **DOI:** 10.1088/1674-1056/ac8af7

1. Introduction

In conventional computers based on semiconductor p–n junctions, the resistance of interconnecting components is the main cause of power consumption.[1] Quantum computers made of superconducting quantum bit with zero dissipation and near-quantum limit sensitivity are the most promising candidate to overcome the shortcoming.[2–8] As a result, the artificial superconductor–semiconductor (SSm) heterojunction at nanometer level as a basic structure for superconducting computing element has turned into the widespread international research frontier and hotspot.[11–15] Remarkable results have emerged in the studies of SSm junctions from many aspects.[16–18]

Previously, unconventional magnetoresistance has been reported in SSm junction such as Ni/Nb heterojunction.[22] In the hetero-structure of superconductor NbN and two-dimensional electron gas (2DEG) $Al_{0.7}Ga_{0.3}Sb$/InAs, it has been found that proximity-induced pseudo-superconductivity can influence the critical current I_c.[23] More recently, non-trivial topological phases and Majorana bound states in low-dimensional SSm systems at the interface[26] have been observed. The above results suggest that integrated superconductor and semiconductor thin films at nano-level will play an important role both for fundamental research as well as practical applications.

In this paper, we report our work on ultrathin Nb films (estimated 8 nm thick) on heavily doped Si substrates. A NbSi SSm heterojunction has been fabricated by electron beam lithograph and reactive ion etching. Transport measurements have been done at different temperatures and magnetic fields. We have observed an abnormal magnetoresistence effect similar to the giant magnetoresistance effect (GMR) when the ultrathin Nb film of the junction is superconducting. The resistance peak is maximal at zero magnetic field, and it rapidly decreases upon increasing magnetic field until reaching a saturation value. A simple model based on the superconductor–barrier layer–superconductor construction formed at the NbSi interface is proposed to understand the origin of this effect.

2. Experimental setup

To obtain the SSm heterojunction, we used heavily doped 1×1 μm^2 n^+ Si (100) as the substrate and an ultrathin polycrystalline-structure superconducting Nb film with a thickness of approximately 8 nm was deposited in a high vacuum (up to 0.6×10^{-7} Pa) DC magnetron sputtering apparatus at 300 K. The substrate was cooled with deionized water during the whole growth process to prevent inter-diffusion and ensure the high quality of the Nb film. Four-probe configuration electrodes with a central area of 60×60 μm^2 were then fabricated on the Nb film using standard ultra-violet exposure technique and reactive ion beam etching (RIE). The final desired heterojunction pattern was achieved in the central region of the electrodes by electron beam lithography and RIE. Transport measurements were carried out in a physical property measurement system (PPMS-9) by Quantum Design equipped with a LS370 AC bridge, a model 6221 current source and

[†]Corresponding author. E-mail: 2381956704@qq.com

© 2023 Chinese Physical Society and IOP Publishing Ltd

a model 2182A nanovoltmeter. The superconducting critical temperature (T_c) is defined as the temperature corresponding to 90% of the normal state resistance R_N.

The morphology of the superconductor–semiconductor heterojunction (hereinafter abbreviated briefly as NbSi junction) has been observed using scanning electon microscopy (SEM), the result is presented in Fig. 1(a). The wide gap etched in the middle separates the film forming a heterojunction structure, the surfaces of the ultrathin Nb films on both sides of the NbSi junction are smooth and uniform. It can be clearly seen that the sidewall of the 1 μm wide gap etched by RIE is very sharp, together with the pronounced boundary between the Nb film and the Si substrate both indicating the high quality of the NbSi junction. Nevertheless, there are some impurities or defects inside the gap shown as bright spots, which are most probably caused by contamination adsorbed in ambient atmosphere.

The resistance–temperature (R–T) curve of the Nb/Si junction is presented in Fig. 1(c). The low junction resistance indicates good electron transparency. After the film enters the superconducting state, the Nb/Si junction resistance decreases slightly at first, then it increases dramatically upon cooling down. The corresponding T_c (4.98 K) of the Nb/Si junction is a little bit lower than that of the ultrathin Nb film and the superconducting broadening is much larger than that of the film, which is mainly due to the degeneration of superconductivity caused by the formation of the heterojunction, surface oxidation or damage induced during the etching and measuring procedure. We also notice that there exists a small resistance rise near T_c in the R–T curve of the ultrathin Nb film and an inflection point in the Nb/Si junction, which will be discussed later.

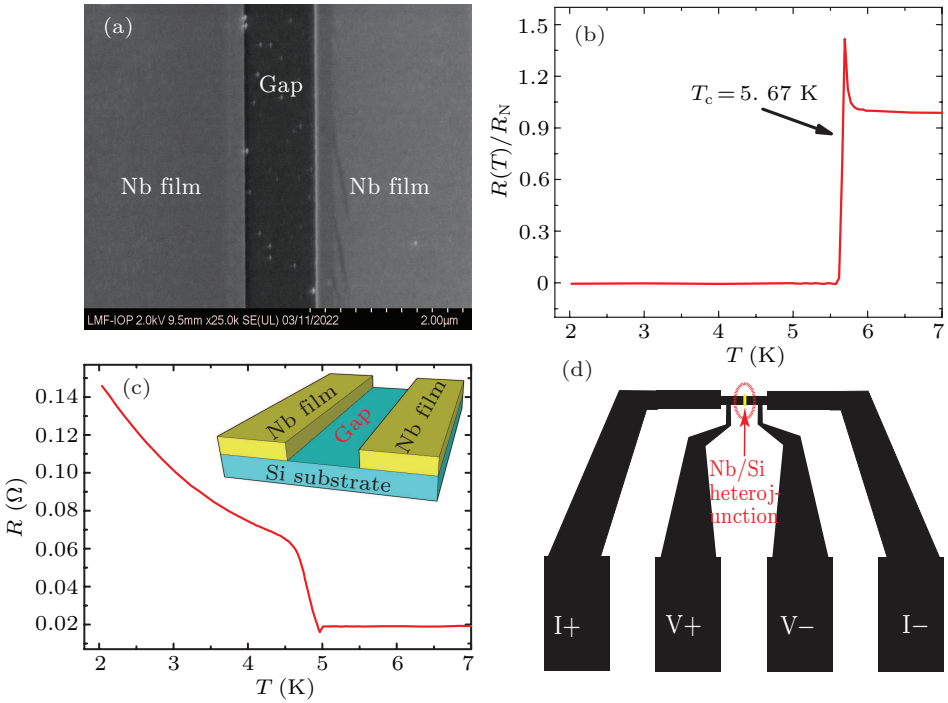


Fig. 1. (a) A representative scanning electron microscope (SEM) image of the ultrathin Nb film with a etched gap of about 1 μm in width, i.e., a typical SEM morphology of the Nb/Si heterojunction. (b) The resistance versus temperature (R–T) curve of the ultrathin Nb film that has not been experienced microfabrication process reveals a T_c of 5.67 K. (c) The R–T curve of our Nb/Si superconductor–semiconductor heterojunction has a slightly smaller T_c at 4.98 K. The inner illustration shows a schematic view of the heterojunction structure of the red circle area in (d). (d) Configuration of the Nb/Si heterojunction, where the red circle is the region where the Nb/Si heterojunction is located, and the yellow line indicates the location of the etched gap.

3. Results and discussion

Figure 2(a) shows the variation curves of the resistance (R) of the Nb/Si junction as a function of temperature (T) and external magnetic field (H) applying perpendicular to the interface. The curves are all symmetric for forward and reverse magnetic fields with a maximum value at zero field, forming a remarkable resistance peak. It is clear that the curves at different temperatures follow the same trends: the resistance decreases rapidly with increasing magnetic field, after reaching the lowest point, there emerges a small resistance-rise section, finally the resistance reaches a plateau after the Nb/Si junction enters the normal state. Following the GMR of the multilayer magnetic thin film system, we define the magnetic field at which the resistance reaches a plateau to be the saturation magnetic field (H_s) at that temperature. It is obvious that the zero-field resistance peak and the H_s are approaching zero upon increasing temperature until both disappear in the normal state of $T > T_c$. Besides the zero-field resistance peak, when coming close to H_s, two weak resistance minimum valleys on both sides of the peak are present. They gradually move to zero but become more pronounced with increasing temperature, eventually vanish at 5 K when the junction is still

superconducting. The resistance change factor from zero to H_s is remarkably large, e.g., at $T = 2$ K the corresponding one is up to 8 times of R_N (here with $H > H_s$).

Figure 2(b) is normalized by the resistance at zero magnetic field for a better view of the MR in Fig. 2(a). Also, the resistance change ratio from zero field to H_s declines with increasing temperature and disappears in the normal state of $T > T_c$. It is surprising that the Nb/Si junction resistance descends by about 85% maximally, while the corresponding maximum value is 50% in the traditional GMR of the Fe/Cr superlattice,[25] and it is well consistent with the result in Fig. 1(c). The H_s of our heterojunction is basically the same as that of Fe/Cr superlattice in value, but it is more sensitive to magnetic field. Finally, from Figs. 2(a) and 2(b) one could find that the line shape of the falling part in the *R*–*H* curves changes significantly with the increasing magnetic field. The inflection point shifts to lower field with temperature going up and only exists at low temperature when the Nb/Si junction is in the superconducting state, and fades away at 4 K before the film enters the normal state. Furthermore, there are some discrepancies between the *R*–*H* platforms at 5 K and 6 K in Fig. 2(b), roughly 2%. The reason is as follows: the Nb/Si junction has not fully reached the normal state at 5 K (our critical temperature criterion is 90% R_N (6 K)) which can be obviously verified from Fig. 1(c), as a result some Cooper pairs remain in the Nb/Si junction. Due to the residual weak superconducting electron pairs, the resistance variation at 5 K is a bit higher than that induced by system noise at 6 K when the junction is in a completely normal state. It means that the difference between 5 K and 6 K can be treated as environment noise, and thus can be neglected. The above-discussed AMR effect together with its evolution characteristics was confirmed on several SSm heterojunction samples.

In order to exclude influence from other unrelated factors, the temperature dependent *R*–*H* results of the ultrathin Nb film before microfabrication are shown in Fig. 2(c). The sharp superconducting transition and small broadening indicate the high quality of the unprocessed ultrathin Nb film. The T_c (0 K) of the film is 5.67 K, consistent with the value obtained in Fig. 1(b). For comparison with the definition of T_c, we define the magnetic field corresponding to 90% of the R_N (high-filed normal-state value here refers to 2.75 T) as the upper critical magnetic field (H_{c2}) of the Nb film. The H_{c2} decreases with increasing temperature and ultimately becomes zero in the normal state, which is a typical behavior of traditional BCS[26] superconductors. Similar to the *R*–*T* shown in Fig. 1(b), the *R*–*H* curves of the ultrathin film also exist a small resistance rise interval near T_c. Moreover, it is quite obvious that the films in the superconducting state exhibit zero resistance and fully diamagnetic, without any sign of AMR emerging in the Nb/Si junctions. After entering the normal state, the curves become a constant straight line that does not vary with the magnetic field.

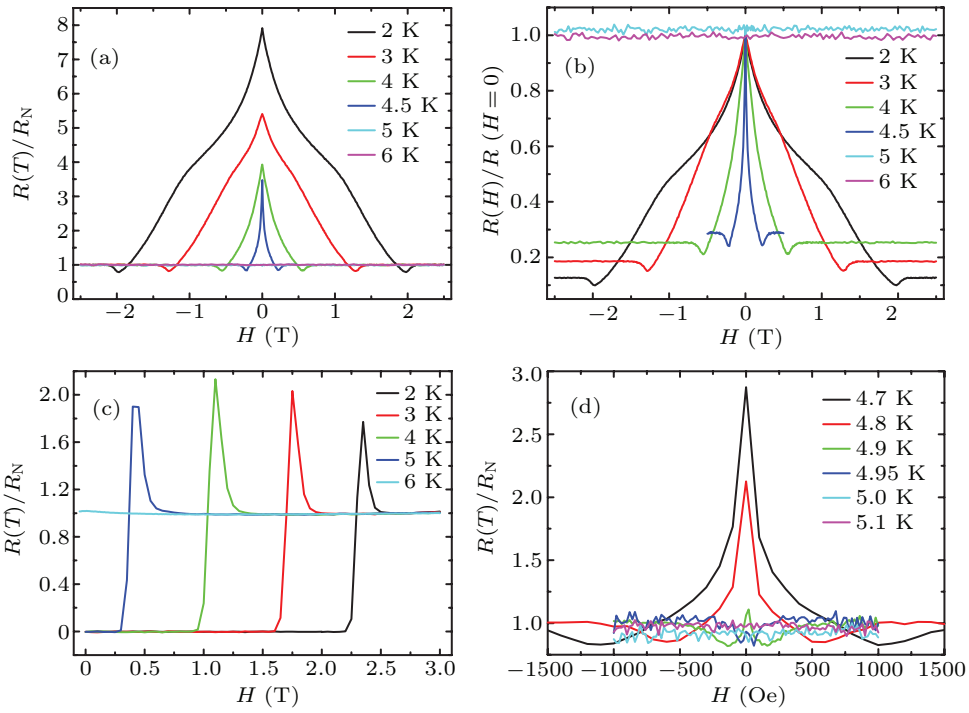


Fig. 2. The applying direction of the magnetic field is perpendicular to the Nb/Si junction interface or the unprocessed ultrathin Nb film and the vertical scale is normalized for clarity. (a) Magnetoresistance of the Nb/Si junction at different temperatures with vertical axis relative to the normal-state resistance value in high-field condition. (b) Close-up views of the magnetoresistance curves in (a) normalized using the zero-field resistance. No abnormal magnetoresistance signature shows up when the film is in the normal state. (c) The temperature-dependent *R*–*H* curves of the ultrathin Nb film normalized by R_N (2.75 T) that has not been undergone any treatment. (d) The zoomed-in results of the *R*–*H* curves of the Nb/Si junction near T_c for better understanding.

Figure 2(d) depicts more details of the R–H curves of the Nb/Si junction around T_c with the vertical axis normalized with R_N ($H > H_s$). It can be immediately seen that as the temperature increases, the peak-shaped zero-field resistance maximum gradually goes down until it fades away above 4.95 K, the two symmetrical resistance minimums on both sides of the peak approach to zero and merge together at last. As a result, the zero-field resistance peak evolves into a minimum valley lower than the normal state plateau at 4.95 K. When $T > 5.0$ K, the unusual behavior of the Nb/Si junction vanishes with the R–H curve becoming a basically unchanged straight line. The data here clearly implies that the Nb/Si junction resistance near T_c is rather sensitive to temperature, a small change in temperature (0.1 K) will induce several times change in resistance. It is also noticed that when scanning the magnetic field at 4.9 K, the position of resistance peak is accidentally offset by about 20 Oe to zero point. It can be attributed to the magnetic vortices trapped in the ultrathin Nb film of the heterojunction. Consequently, there exists a rather small hysteresis in the R–H curve near T_c with different scan directions which could barely been distinguishable and it contributes nothing to the AMR. The characteristic that the resistance reaches a tiny rising stage after the minimum value and ultimately reaches saturation has a certain application in the field of functional sensor detection.[27,28] According to the above discussion, we can definitely conclude that the reported AMR comes from the Nb/Si junction rather than the ultrathin Nb film.

To further investigate the role of low-dimensional nanosuperconductivity in the abnormal magnetoresistance effect, we also carried out differential resistance (dV/dI) measurements, and the data obtained are presented in Fig. 3(a). Due to the relatively small junction resistance, the measurement noise in dV/dI curves is relatively large. The basic line shape is analogous to the tunneling spectrum of superconductor tunnel junction described by BCS theory.[26] At 5.0 K, the superconducting coherence peak still exists, this is consistent with our previous interpretation for the MR difference between 5 K and 6 K in Fig. 2(b). It is quite surprising that Fig. 3(b) clearly shows that the H_{c2} of the ultrathin Nb film is slightly higher than the H_s of the Nb/Si junction at the same temperature, in agreement with the results of T_c in Figs. 1(b) and 1(c). It means that when the magnetic field is between H_{c2} and H_s, although the Nb film is in the superconducting state, the abnormal magnetoresistance of the Nb/Si junction has already disappeared. Furthermore, we found that the difference between H_{c2} and H_s is about 8% of H_{c2} at 2 K, but shows a little upward trend with increasing temperature, which is clearly illustrated by the right axis in Fig. 3(b).

Moreover, we analyzed the data of H_{c2} and H_s using the classical experimental formula

$$H(T) = H(0\ \mathrm{K})\left[1 - \left(\frac{T}{T_c}\right)^2\right], \tag{1}$$

where T_c is the superconducting critical temperature, the results are shown in Fig. 3(c). It can be clearly seen that the experimental data and theoretical fitting are in good agreement, the H_{c2} and H_s both follow the conventional law of superconductivity. Through fitting we got $H_{c2}(0\ \mathrm{K}) = 2.56$ T and $H_s(0\ \mathrm{K}) = 2.49$ T. The degeneration in critical field and T_c of the Nb/Si junction is mainly due to the defects or damage induced in the preparation process. Figure 3(d) shows the change ratio and percent of the Nb/Si junction resistance from zero field to H_s. Obviously, there is an inverse proportional relationship between them, so here we only need to focus on the former. The normal state resistance is basically unchanged, yet the resistance change factor in the superconducting state has a large variation. The change rate at $T < 4.5$ K is lower than that above 4.5 K, which matches the inflection point of the $R(T,H)$ curves in Figs. 2(a) and 2(b). In the range of $T < 4.5$ K, the change rate is highly sensitive to the temperature, once again verifying the results in Fig. 2(d).

We briefly discuss the inflection point in $R(T,H)$ curves of the Nb/Si junction and the small resistance rise near T_c in $R(T,H)$ curves of the ultrathin Nb film. As shown in Fig. 1(c), we define the inflection point temperature T_{gd} at which the slope changes dramatically in resistance drop section when the Nb/Si junction is superconducting. The R–T curve can be divided into four regions by temperature: (1) 2 K (lowest temperature measured)–T_{gd}, (2) T_{gd}–T_{up} (at which the resistance begins to rise), (3) T_{up}–T_c and (4) T_c–7 K (the latter metallicity curve is not of interest). Regions (2) and (3) are mostly linear, similarly the R–H curves in Figs. 2(a) and 2(b) can also be divided into four but almost all nonlinear ones. The T_{gd} moves to lower temperature with increasing magnetic field and disappears at 4 K while the heterojunction is still in the superconducting state. Accordingly, it is speculated that the inflection point may be ascribed to the defects or damage at the junction interface, further studies on the inflection point are needed.

Besides, there is also a small increase near T_c in $R(T,H)$ curves of the ultrathin Nb film shown in Figs. 1(b) and 2(c). The maximum resistance rise is approximately 2.0 times of $R_N(6\ \mathrm{K})$, and its existence temperature range is quite narrow, for example that is only 0.15 K at $T = 2$ K. That resistance rise may be caused by non-uniform current distribution and this distribution will lead to the appearance of this resistance rise. Also it may be because of the two-dimensional superconductivity: the magnetic fluxs trapped by defects inside the film are released from the bound state at T_c and that quantity change of magnetic fluxs leads to the resistance rise. Unfortunately, there is no convincing conclusion about the micro-

physical mechanism behind this resistance rise part and similar phenomenon has been found in thin films.[29,30] That small rise which happens right before T_c does not contribute to the abnormal magnetoresistance which occurs when the ultrathin Nb film is in the superconducting state. The inflection point is the refinement structure of the $R(T,H)$ curves and always emerges when the Nb/Si junction is superconductive, so does the small resistance rise near T_c for the ultrathin Nb films. Satisfactory interpretation for the above two strange features still remains unestablished, more extensive experimental and theoretical works are needed.

The abnormal magnetoresistance effect (AMR) of the Nb/Si junction survives when the ultrathin Nb film is superconductive, whereas the Nb film alone is perfectly zero resistance and fully diamagnetic without any sign of AMR. The small resistance increase around T_c in the ultrathin Nb film is much smaller than that of AMR. Through the previous analysis, we ruled out the influence of the Nb film on this effect. It is clear that AMR comes from the interface superconductivity. Here, we propose a possible qualitative explanation for AMR on the basis of previous work and the electronic structure of heterojunction. The structural configuration we used is shown in Fig. 4(a): there exists semiconductor Schottky barrier,[31,32] Fermi velocity mismatch or damage at the interface, which acts as a barrier layer (the red thin layer between Nb and Si layers), thereby forming the SIN junction structure of superconductor–insulator layer (barrier)–normal metal. Figure 4(a) also is a simplified schematic of the Nb/Si junction equivalent of two SIN junctions, where excitation current I_f flows through both of them. However, the Nb/Si junction is not simply an ideal SIN junction. The transport results include the contribution of two SIN junctions from both sides, i.e., the properties we got reflect the average outcome of these two junctions indeed. We simply consider that the physical parameters of the two junctions are totally identical, so that they can be briefly equivalent as one SIN junction to simplify our description.

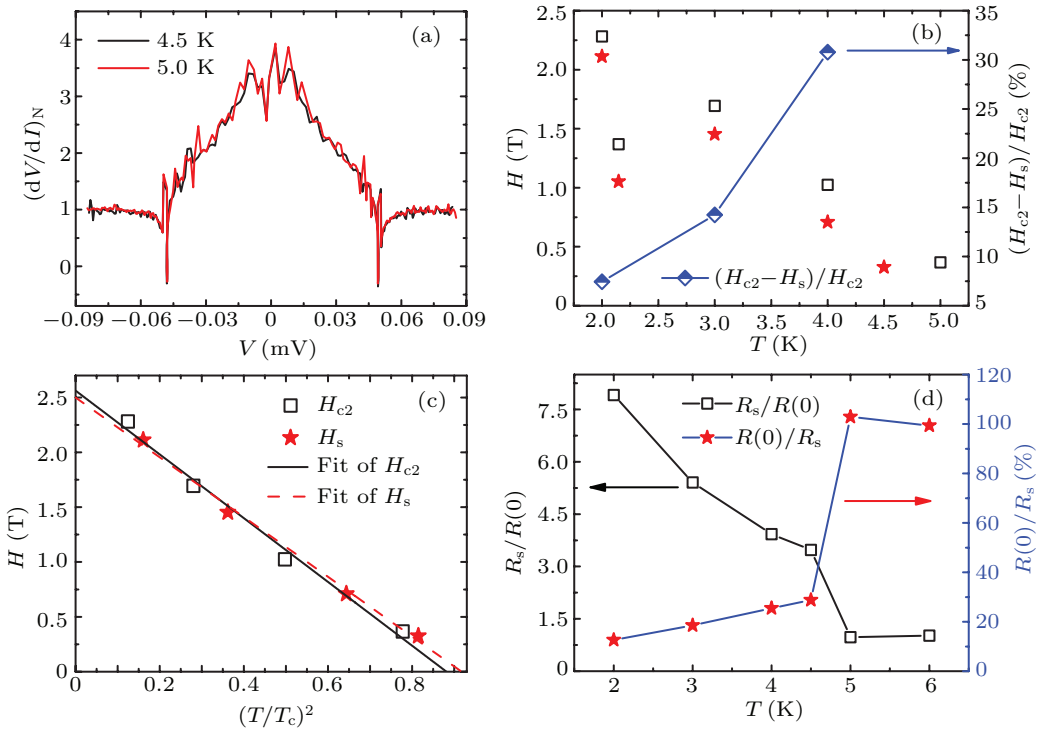


Fig. 3. (a) Partial experimental results of differential resistance dV/dI of the heterojunction normalized using the normal state value at indicated temperatures, i.e., the reciprocal of differential conductance dI/dV. (b) The temperature dependence of the upper critical magnetic field H_{c2} of the ultrathin Nb film and the saturation magnetic field H_s of the Nb/Si junction referring to the left axis. The right side is the discrepancy between them relative to H_{c2} at particular temperatures. The connection between the data points is only for better observation of the changing law. (c) Data points and lines of fitting H_{c2} and H_s through the empirical formula are markedly displayed in the graph. (d) Variation on change ratio and percentage of the Nb/Si junction resistance from zero field to H_{c2} as a function of temperature with the solid line being merely for the convenience of observing.

First, we think about the earlier analysis process of the H_{c2}, H_s and dV/dI. It can be witnessed from Fig. 3(c) that the superconductivity of Nb/Si junctions is well described by classic empirical formula. The line form of dV/dI curve is consistent with the tunneling spectrum of superconductors under BCS theory. Therefore, it is speculated that the AMR might be induced by the electron tunneling at the Nb/Si junction interface according to the phenomenal semiconductor model, as shown in Fig. 4(b) which is the micro-physical mechanism used by Giaever to describe the microscopic process of single electron tunneling.[33,34] The density of states (DOS) of superconductor $N_s(E)$ and normal metal $N_n(0)$ is determined

by the following formula:

$$N_{\rm s}(E)=\begin{cases} N_{\rm n}(0)\frac{E}{\sqrt{E^2-\Delta^2}}, & (E>\Delta),\\ 0, & (E<\Delta), \end{cases} \tag{2}$$

where E is the energy of electron using Fermi energy as a baseline, $N_{\rm n}(0)=\frac{1}{4\pi^2}(\frac{2m}{\hbar})^{\frac{3}{2}}\varepsilon^{\frac{1}{2}}$. It can be seen that the Fermi energies on both sides are identical, and there is no single electron state inside the gap on the right, and only Cooper pairs could exist. Namely, electronic tunneling in the SIN junction forms the current in the heterojunction (tunneling between Nb film and Si substrate), and an increase of the external magnetic field suppresses superconductivity, leading to the decrease of Δ. It can be concluded that both DOS and probability of electron tunneling are enhanced, which is manifested as an increase in the current macroscopically. The stronger the magnetic field, the more significant this effect, so the Nb/Si junction resistance decreases with increasing magnetic field. But this physical picture is too simplistic to interpret the fine structures of the MR curve such as the small resistance rise near $H_{\rm s}$, the difference between $H_{\rm c2}$ and $H_{\rm s}$ or the inflection point in the R–H curves.

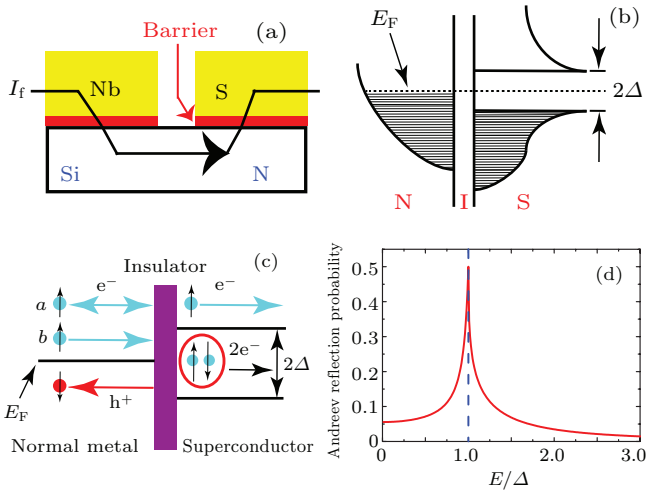


Fig. 4. (a) Sectional view of the Nb/Si junction with the middle red part representing the barrier layer (enlarged for clarity). The equivalent double SIN junctions formed on both sides of the etched gap in the Nb/Si junction where $I_{\rm f}$ represents the current flow direction. N, I and S stand for normal metal (heavily doped Si substrate), insulator (barrier layer) and superconductor (ultrathin Nb film), respectively. (b) Energy band distribution diagram of the phenomenal semiconductor model used by Giaever to understand the junction tunneling process under thermal equilibrium at 0 K. (c) Normal reflection, Andreev reflection, and single electron tunneling process happen when the electrons carrying different energy incident at the SIN junction interface from left. Fermi levels on both sides are at the same level in (b) and (c). (d) The variation of Andreev reflection probability with electron incident energy under BTK theory. The horizontal axis is normalized by the superconducting energy gap Δ.

The most suitable explanation is acquired by considering the Andreev reflection[35,36] at the interface, as shown in Fig. 4(c). In order to simplify the discussion, only the Andreev reflection process that takes place at the interface when the incident electron with energy below Δ is considered, the rest of normal reflection and tunneling processes are ignored. As mentioned previously, we still concentrate on the SIN junction formed at the interface. The heterojunction resistance is very small, so it is believed that the strength of the subsistent barrier layer in the middle of SIN junction is in an intermediate state (right between zero and a strong barrier). With the help of BTK[37] and point contact[38] theory, a dimensionless parameter (Z) is introduced to characterize the strength of the barrier layer at the interface. The SIN junction degenerates into an SN junction with condition that Z is zero. The transport characteristics of the SN junction in this case is the novel conductance doubling owing to the Andreev reflection in the superconducting state. On the other hand, when the Z is high enough (usually greater than 10), the classic Giaever tunneling dominates the transport process of the SIN junction. The more realistic situation is somewhere in between the two states above, i.e., $0<Z<10$. According to the BTK theory, the Andreev reflection probability $A(E)$ depending on the electron energy E is written as

$$\begin{cases} A(E)=\frac{\mu_0^2\nu_0^2}{\gamma^2}, \\ \mu_0^2=1-\nu_0^2=\frac{1}{2}\left(1+\sqrt{\frac{E^2-\Delta^2}{E^2}}\right), \\ \gamma=\mu_0^2+(\mu_0^2-\nu_0^2), \end{cases} \tag{3}$$

where Δ is the superconducting energy gap, μ_0^2, ν_0^2, γ are parameters in the derivation of the BTK theory, and the results are shown in Fig. 4(d). When the electron energy changes from zero to Δ, $A(E)$ grows quickly. After the energy gap is exceeded, $A(E)$ decreases rapidly as the electron energy increases further. Applying magnetic field suppresses superconductivity of the Nb/Si junction, the energy gap decays consequently. So the electron energy is much more accessible to Δ relatively. Still using the phenomenological semiconductor model in Fig. 4(b), we know that as the electron energy becomes close to Δ, the DOS in superconductor $N_{\rm s}(E)$ and normal metal $N_{\rm n}(0)$ near Fermi surface both increase gradually. According to the definition of current, $I\propto N_{\rm s}(E)N_{\rm n}(0)A(E)$, thereby with magnetic field increasing, the increase in both the $A(E)$ and DOS leads to decrease in the resistance of the Nb/Si junction effectively. Exactly at the energy gap, the $A(E)$ has a maximum value, which corresponds to the minimum valley of the magnetoresistance curves. In this way, the evolution of the Nb/Si junction resistance in the process of increasing magnetic field from zero to $H_{\rm s}$ is qualitatively understood. However, this model also has some disadvantages of its own, it cannot be applied to explain the inflection point in the $R(T,H)$ curves at this stage. That may potentially be the result of some weak superconductivity due to the superconducting proximity effect in the barrier layer which is in a competitive relationship with the Andreev reflection. We need more detailed quantitative calculation results extensively, which is our next target in the following days.

Besides the above proposals, according to the inflection point in the resistance decline interval of the $R(T,H)$ curves, inspired by the possible theoretical model of the pseudogap of high-T_c superconductors, we think that the abnormal behavior in the Nb/Si junction seems to be a result of competition between two different microcosmic interactions. The slope of the $R(T,H)$ curves changes significantly on both sides of the inflection point, which can be considered as one different interaction playing a dominant role on each side. As for these two mechanisms, they are most likely associated with semiconductor carrier properties and superconductivity at the interface.

4. Conclusion

To summarize, an abnormal magnetoresistance effect has been observed in superconductor–semiconductor heterojunctions composed of nanosized superconducting Nb films and heavily doped Si substrates. A simple model based on the superconductor–barrier layer–superconductor construction formed at the NbSi interface is proposed to understand the origin of this effect. The columnar-crystal structure of nanoscale ultrathin-superconductive films that suppresses superconductivity and greatly modulates the electronic structure around the Fermi surface could be highly possible to play an important role. The abnormal MR in SSm heterojunctions is quite similar to the GMR effect of magnetic thin films that can be exploited in the development of magnetic storage, magnetic field switching,[39,40] and sensors with high sensitivity. This effect obtained comes from the electron transport across the interface between superconductor Nb film and semiconductor Si substrate, so it can be well compatible with the modern microelectronic semiconductor manufacture technology, and it is of great interest to further explore this effect.[41–44]

Data availability statement

The data that support the findings of this study are openly available in Science Data Bank at http://doi.org/10.57760/sciencedb.j00113.00048.

Acknowledgements

Z.W.H. acknowledges the financial support from the National Natural Science Foundation of China and the Ministry of Science and Technology of China. And we are also very grateful for the useful discussions with Prof. Bing Xu from the Institute of Physics, Chinese Academy of Sciences.

References

[1] Hecht J 1989 *AIP Computers in Physics* **3** 34
[2] Makhlin Y, Schön G and Shnirman A 2004 *Nature* **431** 138
[3] Chiorescu I, Nakamura Y, Harmans C M and Mooij J 2003 *Science* **299** 1869
[4] Wendin G and Shumeiko V S 2001 *Science* **292** 231
[5] Martinis J M, Nam S, Aumentado J and Urbina C 2002 *Phys. Rev. Lett.* **89** 117901
[6] Yu Y, Han S Y, Chu X, Chu S I and Wang Z 2002 *Science* **296** 889
[7] Spethmann M, Zhang X P, Klinovaja J and Loss D 2022 arXiv:2205.03843v1
[8] Rieger D, Günzler S, Spiecker M, Paluch P, Winkel P, Hahn L, Hohmann J K, Bacher A, Wernsdorfer W and Pop I M 2022 arXiv:2202.01776v1
[9] Becerra V F, Trif M and Hyart T 2022 arXiv:2206.03527v1
[10] Nguyen H Q, Sabonis D, Razmadze D, Mannila E T, Maisi V F, Zanten D M T, O'Farrell E C T, Krogstrup P, Kuemmeth F, Pekola J P and Marcus C M 2022 arXiv:2202.05970v1
[11] Mikkelsen A E G, Kotetes P, Krogstrup P and Flensberg K 2018 *Phys. Rev. X* **8** 031040
[12] Hertel A, Eichinger M, Andersen L O, van Zanten D M T, Kallatt S, ScarlinoP, Kringhøj A, Chavez-Garcia J M, Gardner G C, Gronin S, Manfra M J, Gyenis A, Kjaergaard M, Marcus C M and Petersson K D 2022 arXiv:2202.10860v1
[13] Carrad D J, Stampfer L, Olšteins D, Petersen C E N, Khan S A, Krogstrup P and Jespersen T S 2022 arXiv:2205.03217v1
[14] Takayanagi H and Kawakami T 1985 *Phys. Rev. Lett.* **54** 2449
[15] Eroms J, Weiss D, Boeck J D, Borghs G and Zulicke U 2005 *Phys. Rev. Lett.* **95** 107001
[16] Lutchyn R M, Bakkers E P A M, Kouwenhoven L P, Krogstrup P, Marcus C M and Oreg Y 2018 *Nature Reviews Materials* **3** 52
[17] Wang J, Ma X C, Qi Y, Fu Y S, Ji S H and Lu L 2007 *Appl. Phys. Lett.* **90** 113109
[18] Wang J, Ma X C, Lu L, Jin A Z, Gu C Z, Xie X C, Jia J F, Chen X and Xue Q K 2008 *Appl. Phys. Lett.* **92** 233119
[19] Barber, Jr. B P, Hsu S Y, Valles, Jr. J M, Dynes R C and Glover III R E 2006 *Phys. Rev. B* **73** 134516
[20] Bhatia E, Hussain Z, Reddy V R, Barber Z H and Senapati K 2021 *J. Phys.: Condens. Matter* **33** 295803
[21] Akazaki T, Yamaguchi H, Nitta J and Takayanagi H 1999 *Supercond. Sci. Technol.* **12** 901
[22] Moshchalkov V V, Gielen L, Strunk C, Jonckheeret R, Qiu X, Haesendonck C V and Bruynseraede Y 1995 *Nature* **373** 319
[23] Bezryadin A, Lau C N and Tinkham M 2000 *Nature* **404** 971
[24] Val'kova V V, Shustina M S, Aksenova S V, Zlotnikova A O, Fedoseeva A D, Mitskana V A and Kaganb M Y 2022 arXiv:2205.10069v1
[25] Baibich M N, Broto J M, Fert A, Dau F N V and Petroff F 1988 *Phys. Rev. Lett.* **61** 2472
[26] Bardeen J, Cooper L N, and Schrieffer J R 1957 *Phys. Rev.* **108** 1175
[27] Irwin K, Hilton G, Wollman D and Martinis J 1996 *Appl. Phys. Lett.* **69** 1945
[28] Day P K, LeDuc H G, Mazin B A, Vayonakis A abd Zmuidzinas J 2003 *Nature* **425** 817
[29] Crusellas M A, Fontcuberta J and Piñol S 1992 *Phys. Rev. B* **46** 14089
[30] Kunchur M, Zhang Y Z, Lindenfeld P and McLean W L 1987 *Phys. Rev. B* **36** 4602
[31] Tung R T 1984 *Phys. Rev. Lett.* **52** 461
[32] Heslinga D R, Weitering H H, Van der Werf D P, Klapwijk T M and Hibma T 1989 *Phys. Rev. Lett.* **64** 1589
[33] Giaever I 1960 *Phys. Rev. Lett.* **5** 147
[34] Giaever I 1960 *Phys. Rev. Lett.* **5** 464
[35] Andreev A F 1964 *Sov. Phys. JETP* **19** 1228
[36] Pannetier B and Courtois H 2000 *Journal of Low Temperature Physics* **118** 599
[37] Blonder G E, Tinkham M and Klapwijk T M 1982 *Phys. Rev. B* **25** 4515
[38] Daghero D and Gonnelli R S 2010 *Supercond. Sci. Technol.* **23** 043001
[39] Adachi K, Suzuki T, Kato K, Osaka K, Takata M and Katsufuji T 2005 *Phys. Rev. Lett.* **95** 197202
[40] Kapran O M, Morari R, Golod T, Borodianskyi E A, Boian V, Prepelita A, Klenov N, Sidorenko A S and Krasnov V M 2022 arXiv:2205.01534
[41] Leggett A J 2002 *Science* **296** 861
[42] Devoret M H and Schoelkopf R J 2013 *Science* **339** 1169
[43] Barends R, Shabani A, Lamata L, *et al*. 2016 *Nature* **534** 222
[44] Banerjee D 2022 arXiv:2203.14836v1